Characterization and Analysis of Gate and Drain Low-frequency Noise in AlGaN/GaN HEMTs

Shawn S.H. Hsu, Pouya Valizadeh, Dimitris Pavlidis
Department of Electrical Engineering and Computer Science,
The University of Michigan, Ann Arbor, MI 48109-2122, USA
J. S. Moon, M. Micovic, D. Wong and T. Hussain
HRL Laboratories, 3011 Malibu Canyon Road, Malibu, CA 90265, USA

Abstract

The gate and drain low-frequency noise (LFN) characteristics of 0.15×200 μm^2 AlGaN/GaN HEMTs are reported. The measured gate noise current spectral density is low and insensitive to the applied high reverse bias voltage between the gate and the drain. Typical gate noise level values vary from ~ 1.9×10^{-19} to ~ 3.4×10^{-19} (A^2/Hz) as the drain voltage increases from 1 V to 12 V (V_G= -5V) at 10 Hz. The calculated Hooge parameter is ~ 5.9×10^{-4}, which is comparable to traditional III-V FETs. Lorentz noise components were observed when V_{DS} is higher than 8 V. The peak of Lorentz component moves toward higher frequency when V_{DS} increases and V_{GS} decreases. The exponent γ of the $1/f^{\gamma}$ was found to reduce from 1.17 to 1.01 when V_{DS} increases from 8 V to 16 V. The observed trends are discussed in terms of electric field, carrier velocity and trapping-detrapping considerations.

I. Introduction

GaN-based HEMTs have demonstrated excellent microwave power and noise characteristics [1]. The low-frequency noise (LFN) characteristics of these devices have also attracted significant attention since LFN can be upconverted to microwave frequencies in nonlinear circuits and may lead to circuit performance degradation. In addition, LFN often originates from defects and traps and can be a useful tool to diagnose problems of materials and technologies. LFN and deep-level traps have been reported for GaN-based HEMTs [2], [3]. There is, however, still a need for better understanding and analysis of LFN mechanisms in AlGaN/GaN HEMTs. This paper presents a systematic study of LFN in such devices. Submicrometer gate AlGaN/GaN HEMTs were characterized for both gate and drain noise characteristics under different bias conditions. Section II describes the layer structure and the device DC and microwave characteristics. Section III presents the experimental results of both the gate and drain noise current characteristics. The bias dependence and the origin of LFN were also investigated. Section IV discusses the observed trends of LFN in AlGaN/GaN HEMTs and compares different models.

0-7803-7478/02/$17.00 © 2002 IEEE

II. DC and Microwave Characteristics

The AlGaN/GaN HEMTs tested were grown by RF-assisted MBE on 4H-SiC substrates. An undoped GaN buffer layer was grown on top of the substrate, followed by an undoped AlGaN spacer, an AlGaN barrier layer, and an undoped AlGaN cap layer. The measured device had a gate length of 0.15 μm and a total gate periphery of 200 μm. The peak transconductance was ~ 280 mS/mm and the maximum current capability was ~ 1 A/mm. Typical DC *I-V* characteristics of the device are shown in Fig. 1. The pinch-off voltage of the device is ~ -5.5 V. The positive slope of the *I-V* characteristics in the saturation region results from short-channel effects, which lead in a reduced output resistance. The presence of finite output resistance needs to be considered, and a correction factor was used when calculating the drain noise current from the measured drain noise voltage. Fig.2 shows the maximum oscillation frequency (f_{max}) and cut-off frequency (f_T) under various bias conditions. As can be seen, the maximum oscillation frequency (f_{max}) and cut-off frequency (f_T) were ~ 75 GHz and ~ 50 GHz, respectively.

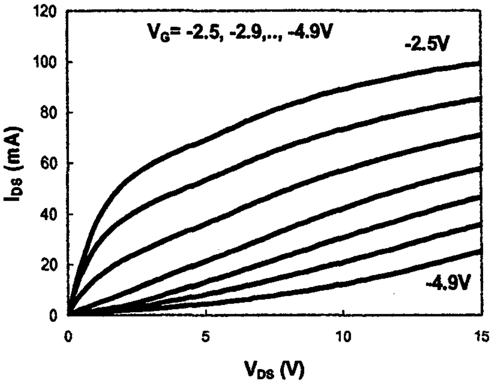

Fig. 1: DC *I-V* characteristics of the investigated 0.15× 200 μm^2 AlGaN/GaN HEMTs.

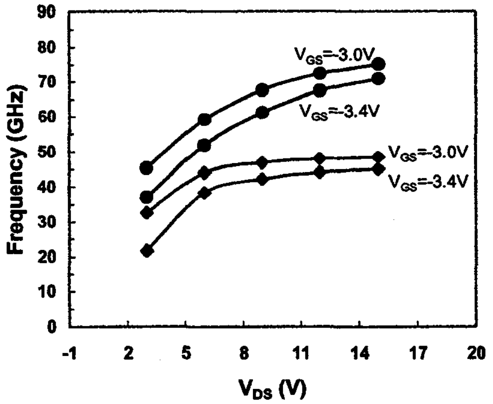

Fig. 2: Maximum oscillation frequency (f_{max}) and cut-off frequency (f_T) under different bias conditions.

III. Low-frequency Noise Characteristics

On-wafer LFN characterization was performed using an in-house developed measurement system. Microwave probes and bias-Tees were used to provide consistent contact and reduce the possibility of oscillation at low frequencies. Batteries were used for biasing to reduce undesired noise sources from the power supply. A low-noise amplifier (LNA) with a gain of ~ 60 dB was used to increase the signal level and an HP3561A analyzer with a high dynamic range was used to collect data. The gate noise was measured when the drain terminal is AC grounded, while the drain noise was measured when the gate terminal is AC grounded. Measurements were performed from 10 Hz to 100 kHz with automatic computer control. The system was calibrated using resistors from their thermal noise values and was placed in a Faraday cage to minimize interference from the environment.

The gate noise current spectral density was first examined under a wide range of bias conditions. Fig. 1 shows the results obtained when the device is biased in the saturation region (V_{DS}= 12 V) under different gate voltages. The gate noise level increases as the gate-drain reverse bias increases due to the increased gate leakage current. The gate noise level changed from 1.93×10^{-19} A^2/Hz to 3.42×10^{-19} A^2/Hz when the drain voltage increased from 1 to 12 V under V_{GS}= -5 V.

The small dependence of the gate noise current on the drain bias voltage can be explained using the Schottky diode noise model. Under reverse bias conditions, the major low-frequency noise source in a Schottky diode is generation-recombination (G-R) noise current originating from the space-charge-region (SCR) and can be associated with the gate leakage current. As a result of the wide bandgap AlGaN layer used as barrier, the gate leakage current increases only slightly even under strong gate-drain reverse-bias conditions. This results in small gate noise current levels and characteristics insensitive to gate-drain reverse bias even under pronounced bias conditions. Measurements of the gate leakage current showed that I_g only increased from ~ 0.2 to ~ 0.5 μA when V_{DS} increases from 1 to 12 V under V_{GS}= -5V, which is consistent with the LFN results. In addition, the small gate noise variation even under a large change of V_{DS} suggests that the devices can be used for large-signal applications with low gate noise level.

Fig. 4 shows the normalized drain noise current spectral density for the devices biased in the linear region (V_{DS}= 0.5 V) as a function of effective gate voltage. The result shows that S_{Id}/I_D^2 reduces monotonically when the effective gate voltage increases. Similar characteristics have been observed in AlGaN/GaN HEMTs from other researchers, and were explained by the screening effect from the high electron density in the channel [4]. When the devices operate close to open-channel conditions, the sheet carrier density increases and Coulomb interaction between scattering centers and channel carriers reduces due to high carrier concentration screening effects. As a result, the electron mobility increases resulting in a reduced noise level. On the contrary, when the devices operate close to pinch-off conditions, the scattering mechanism is enhanced, and a higher noise level was observed.

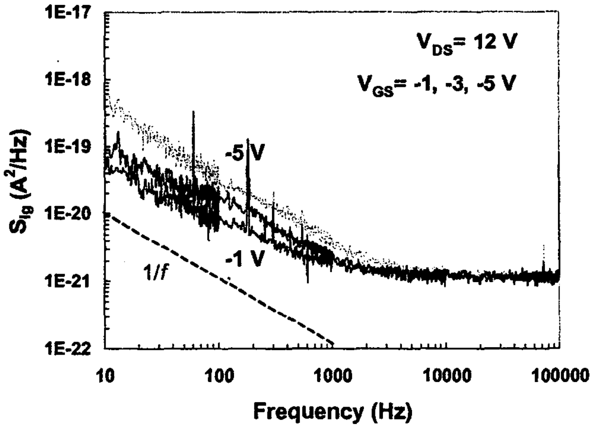

Fig. 3: Gate noise current spectral density of AlGaN/GaN HEMTs biased in the saturation region.

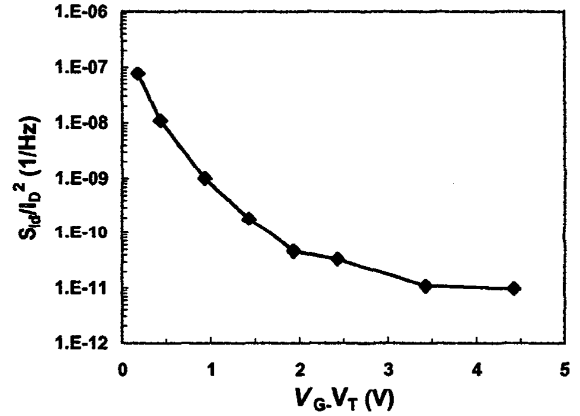

Fig. 4: Normalized drain noise current spectral density for 0.15×200 μm^2 AlGaN/GaN MODFETs at 10 Hz. The drain voltage is 0.5 V.

The Hooge parameter can be calculated using the following equation:

$$\alpha_H = \frac{S_{Id}}{I_{DS}^{\ 2}} f\, N \tag{1}$$

where f is the frequency, N is the total number of carriers. I_{DS} is the drain-source bias current and f is the frequency. The calculated α_H values were 5.9×10^{-4} under V_G= 0 V and V_{DS}= 0.5 V. The obtained values are comparable to those reported in [2] for AlGaN/GaN MODFETs, where $\alpha_H \sim 10^{-4}$ were found under different gate bias voltages.

The obtained values are also close to traditional III-V based FETs, which are normally in the range of ~ 10^{-4} to 10^{-5} [5].

Fig. 5 shows the drain noise current spectral density under various drain voltages. The device presents clear $1/f^{\gamma}$ characteristics with γ ~ 1.05 under low drain bias conditions. However, one can see "bulges" appearing in the $1/f$ characteristics as V_{DS} increases. The bulges shown in the $1/f$ noise characteristics originate from trapping-detrapping and/or generation-recombination (G-R) processes and are often referred to "Lorentz components". As can be seen, the Lorentz components are only present at high drain voltages. It is therefore reasonable to associate the appearance of bulges to the strength of the applied electric field. Under high V_{DS}, the electric field along the submicrometer-gate channel can become extremely high. For example, the electric field can reach ~ 6.67×10^7 V/m at V_{DS}= 10 V for a device with L_g= 0.15 μm. Under such conditions, the carriers may become very energetic, and the trapping-detrapping and G-R processes may be enhanced. Since these processes are very noisy, the Lorentz components become more pronounced. In addition, the observed noise spectral densities show a small curvature, which indicates that the noise occurs from traps with a broad distribution in time constants.

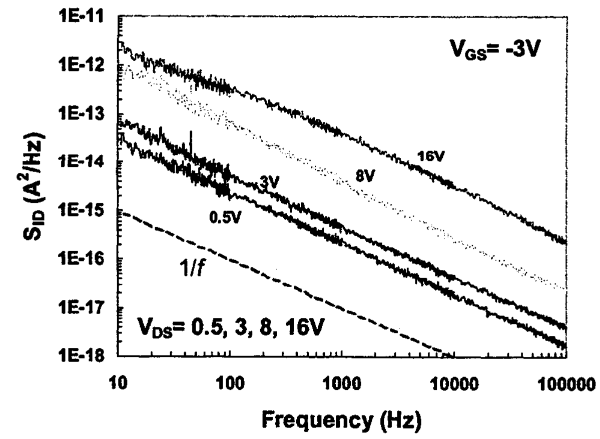

Fig. 5: Drain noise current spectral densities of AlGaN/GaN HEMTs under different drain voltages.

Fig. 6 shows $S_{Id}(f)\times f$ as a function of frequency at V_{GS}= -3V and under different drain voltages. This representation makes a better distinction between the Lorentz components and the $1/f^{\gamma}$ characteristics. The results show noticeable bulges and their peaks move toward higher frequencies as V_{DS} increases. In addition, measurements also show that the peak of Lorentz components move toward higher frequencies when V_{GS} becomes more negative. This can be explained using the modified carrier density fluctuation model, which has been applied to explain LFN characteristics in MOSFETs [6]. The SiO_2/Si structure in MOSFETs can be assumed to be analogous to the AlGaN/GaN structure of the devices under study and therefore a similar theory may be applied. As the drain voltage increases, the band-bending near the drain end between gate and drain reduces. As a result, carriers encounter an increased number of effective traps and reduced carrier-tunneling distance. The latter is due to relatively smaller band-bending which in case of tunneling into the AlGaN spacer leads in less time required for the trapping-detrapping process. Based on this consideration, the bulge peaks are expected to move toward higher frequencies. A similar explanation can be applied to the dependence of the bulges on V_{GS}.

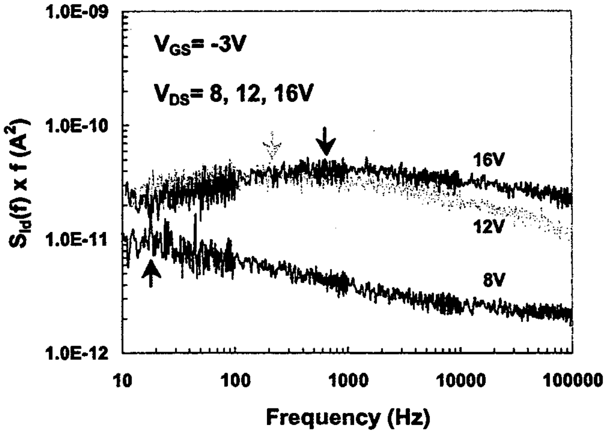

Fig. 6: Product of drain noise current spectral densities and frequencies under different drain voltages.

Fig. 7 shows the bias dependence of γ in saturation region. The γ values were extracted using the $S(f)= A/f^{\gamma}$ equation to fit the measured data, where A is a constant. The device presents a clear trend of reduced γ as the drain voltage increased. γ was found to reduce from 1.17 to 1.01 when V_{DS} increases from 8 V to 16 V. As noted already, the increased drain bias results in relatively smaller band-bending. The time constant needed for the trapping-detrapping process is consequently shortened and a higher noise power appears in the high frequency region, leading in reduction of the γ exponent. Results on the dependence of γ on the bias have already been reported. Balandin *et al.* [2] found for example, that γ decreases from ~ 1.3 to ~ 1.0 when V_{GS} decreases from 0 V to - 6 V. The observed results can also be interpreted using the modified carrier density fluctuation model with band-bending variation as discussed in the next section.

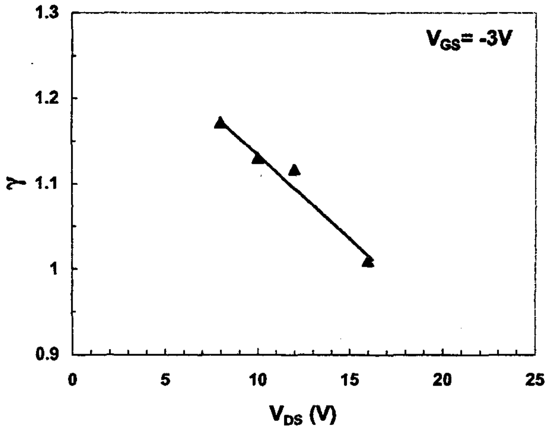

Fig. 7: Dependence of the exponent γ of the $S_{Id}(f)$ $1/f^{\gamma}$ characteristics on V_{DS}. γ reduces when V_{DS} increases.

IV. Discussion

Although the number fluctuation theory provides a more intuitive approach to explain the observed experimental results, the mobility fluctuation model with the activation energy and temperature related time constant can also be used to interpret the experimental results of this work. Ho *et al.* [7] suggested that the dependence of γ on V_{GS} observed in AlGaN/GaN MODFETs is due to the change of trap energy level with respect to the Fermi level in the device, which leads to variation of activated traps in the devices. As a result, the trapping time constants and γ change. γ could increase or decrease depending on the actual distribution of the traps in both real space and energy levels. The number fluctuation model with trapping time constant depending on band-bending appears to be applicable in explaining the experimental results in this study. However, since the trapping time constant is only a function of tunneling distance, this theory is insufficient to describe the $1/f^{\gamma}$ characteristics under different temperatures. On the other hand, the mobility fluctuation model used in [7] where the trap time constants are a function of thermal activation energy does not clearly relate the bias dependence to the $1/f^{\gamma}$ characteristics. Moreover, the LFN characteristics of our study seem to closely relate to the electric field applied along the channel, which will change the carrier velocity and therefore may also impact the trapping-detrapping time constant. This is an aspect that has not been explained extensively since most of reported device characteristics are usually under low drain voltage. A better $1/f^{\gamma}$ noise model including the impact of carrier tunneling distance and activation energy on trapping-detrapping time constants, and the impact of hot carrier effects may therefore be necessary for the analysis of low-frequency noise in AlGaN/GaN MODFETs under high bias conditions.

V. Conclusion

Overall, LFN of AlGaN/GaN HEMTs was investigated for both gate and drain under different bias conditions. The results indicate that the gate noise current was low and insensitive to the gate-drain reverse bias. The normalized drain noise current in the linear region increases as the device is biased close to pinch-off, which can be explained by screening effects. The drain noise current spectral density in the saturation region presented bias-dependent Lorentz components. The observed LFN characteristics are discussed in terms of electric field, carrier velocity and trapping-detrapping considerations. Overall, this study provides further physical understanding of LFN characteristics in AlGaN/GaN HEMTs.

Acknowledgement: Work supported by ONR (contract nos. N00014-00-1-0879, N00014-02-1-0128) and HRL Laboratories. The authors are grateful to Drs. J. Zolper and H. Dietrich for technical discussions and support of this work.

[References]

[1] S. S.H. Hsu, D. Pavlidis, J.S. Moon, M. Micovic, C. Nguyen, D. Grider, "Low noise ALGaN/GaN MODFETs with high breakdown and power characteristics," *IEEE 23rd GaAs IC Symposium*, Baltimore, MD, USA, Oct. 2001, pp. 229-232.

[2] A. Balandin, S. V. Morozov, S. Cai, R.Li, K.L. Wang, G. Wijeratne, and C. R. Viswanathan, "Low Flicker-noise GaN/AlGaN heterostructure field-effect transistors for microwave communications," *IEEE Trans. Microwave theory and tech.*, vol. 47, no. 8, pp. 1413–1417, Aug. 1999.

[3] S. L. Rumyantsev, N. Pala, M. S. Shur, E. Borovitskaya, A. P. Dmitriev, M. E. Levinshtein, R. Gaska, M. Asif Khan, J. Yang, X. Hu, and G. Simin, "Generation-recombination noise in GaN/AlGaN heterostructure field effect transistors," *IEEE Trans. Electron Devices*, vol. 48, No. 3, pp. 530–534, March 2001.

[4] J. A. Garrido, F. Calle, E. Munoz, I. Izpura, J. L. Sanchez-Rojas, R. Li, and K. L. Wang, "Low frequency noise and screening effects in AlGaN/GaN Hemts," *Electronics letters*, vol. 34, No. 24, pp.

[5] M. Tacano, and Y. Sugiyama, "Comparison of 1/f noise of AlGaAs/GaAs HEMTs and GaAs MESFETs," *Solid-state electronics*, vol. 34, no. 10, pp. 1049-1053, Oct. 1991.

[6] Z. Celik and T. Y. Hsiang, "Spectral dependence of $1/f^{\gamma}$ noise on gate bias in n-MOSFETs," *Solid-state electronics*, vol. 30, no. 4, pp. 419-423, 1987.

[7] W.Y. Ho; C. Surya, K.Y. Tong, W. Kim, A. E. Botcharev, H. Morkoc, "Characterization of flicker noise in GaN-based MODFET's at low drain bias," *IEEE Trans. Electron Devices*, vol. 46, No. 6, pp. 1099–1104, June 1999.